The evolutionary dynamics of RNA-guided gene drives

Charleston Noble*, Jason Olejarz*, …, George M. Church & Martin A. Nowak

The genetic manipulation of wild populations has been discussed as a solution to a number of humanity's most pressing ecological and public health concerns, including the eradication of insect-borne diseases such as malaria, the reversal of herbicide and pesticide resistance in agriculture, and the control of destructive invasive species[1,2]. Enabled by the recent CRISPR/Cas9 revolution in genome editing[3], RNA-guided gene drives—selfish genetic elements which can spread through wild populations even if they confer no advantage to their host organism—are rapidly emerging as the most promising approach[2,4–10]. Before this technology reaches real-world application, however, it is imperative to develop a deep theoretical understanding of the potential long-term outcomes of drive release in a wild population. Toward this aim, we here present the first evolutionary dynamics study of RNA-guided gene drives. In particular, we show that drive spread occurs along one of four distinct classes of trajectories—two of which are counterintuitive and previously unreported—and we derive simple conditions based on tunable design parameters which are sufficient to yield evolution toward a desired outcome. Furthermore, our results imply a simple design for 'threshold gene drives' which spread only if released at a sufficiently high initial frequency, providing a practical mechanism for localized containment of gene drive spread[11–13].

Gene drives are selfish genetic elements which bias their own inheritance and spread through populations in a super-Mendelian fashion (Fig. 1a). Various examples can be found in nature, including transposons[14], Medea elements[15], and segregation distorters[16], but so-called

*These authors contributed equally to this work

homing endonuclease gene drives have received the most significant attention in the literature. In general, these function by converting drive-heterozygotes into homozygotes through a two-step process: (1) the drive construct, encoding a sequence-specific endonuclease, induces a double-strand break (DSB) at its own position on a homologous chromosome, and (2) subsequent DSB repair by homologous recombination (HR) copies the drive into the break site (Fig. 1b). Any sequence adjacent to the endonuclease will be copied as well; if a gene is present we refer to it as 'cargo', as it is 'driven' by the endonuclease through the population.

Though originally proposed over a decade ago[1], the chief technical difficulty of this approach—inducing precisely targeted cutting—has only recently been overcome by the discovery and development of the CRISPR/Cas9 system[3,17]. Briefly, Cas9 is an endonuclease whose target site is prescribed by an independently expressed guide RNA (gRNA) via a 20-nucleotide protospacer sequence. Due to the large space of possible 20-nucleotide sequences, virtually any position in a genome can be uniquely targeted by Cas9, and thus so-called RNA-guided gene drives can be constructed simply, requiring only the engineering of a suitable Cas9/gRNA construct[2].

Previous studies have provided experimental proofs-of-concept for endonuclease gene drives in small laboratory populations[4–7,18] or considered the population genetics of gene drives under specific conditions[1,19,20], but none have explored the evolutionary dynamics of gene drives in general. Of particular concern is the potential for emergence of drive resistance within a population, which has not been studied in any depth previously. This can occur if non-homologous end joining (NHEJ) is employed rather than HR in repairing a drive-induced double-strand break; this pathway typically introduces a small insertion-deletion mutation at the endonuclease target sequence, resulting in the creation of a drive-resistant allele rather than the

46 desired duplication of the drive allele (Fig. 1b). Far from an unlikely scenario, NHEJ is strongly
47 favored over HR in many organisms[21–23].

48 To understand the potential behaviors of RNA-guided gene drives, we here consider a
49 genetics-based evolutionary dynamics model. In particular, we study the evolution of a
50 population of diploid organisms and focus on a specific locus which has three alleles, the wild-
51 type (A), the gene drive (D), and a drive-resistant allele (R) which is a loss-of-function variant of
52 the wild-type (Fig. 1b). To abstract the cellular-level drive dynamics, we assume that the wild-
53 type allele in an AD heterozygote is converted to a drive allele with probability P or to a drive-
54 resistant allele with probability 1-P (Fig. 1c). Both the drive and resistant alleles are immune to
55 targeting by the endonuclease and thus are not converted similarly. A simple biological
56 interpretation for P is the chance that double-strand break repair occurs by HR rather than NHEJ,
57 and this varies from as low as $P \approx 0.25$ in mammalian cells[23] to as high as $P \approx 1$ in yeast[5,24].

58 To describe the population-level dynamics of gene drive spread, we assume that gene
59 drive release occurs in an infinite, randomly mating population with viability selection. For the
60 sake of simplicity, we assume that the drive confers a dominant fitness cost c on its host
61 organism, while the resistant allele confers a recessive cost s (Fig. 1d). We consider the former
62 justified by the high cutting efficiency of Cas9 paired with its potential for off-target cleavage[3]
63 and the latter by the relative rarity of dominant loss-of-function mutations[25]. Note that both of
64 these parameters can be tuned when engineering gene drive systems: c can be increased either by
65 including a costly (dominant) cargo gene in the drive construct or by engineering purposeful off-
66 target cleavage, while s can be increased or decreased simply by choosing more- or less-
67 essential genes for targeting by the drive.

Depending on these costs, gene drive release in a population results in one of four long-term behaviors (Fig. 2). Each occurs in a distinct regime in parameter space, and these are separated by simple, linear boundaries: $s=c$ and $c=P/(1+P)$ (Fig. 2a and 2b). The former intuitively divides the space based on whether the drive allele or resistant allele is more costly, while the latter can roughly be thought of as the minimum cost for which the drive no longer achieves super-Mendelian inheritance. To see this, consider an AD heterozygote. If D were to follow standard Mendelian inheritance, then the next generation would inherit it with probability $P_M=1/2$. If, instead, D were a gene drive as described above, then the next generation would inherit it with probability $P_D=(1-c)(1+P)/2$. Super-Mendelian inheritance then requires that $P_D>P_M$, implying that $(1-c)(1+P)>1$, or equivalently, $c<P/(1+P)$.

Two of these regimes, I and IV, produce the expected dynamics. If the drive is fairly neutral and resistance is costly (Regime I), then the drive eventually spreads to fixation (Fig. 2c and Fig. 3a). Resident wild-type populations are susceptible to invasion by infinitesimal initial drive perturbations (SI Sections 3.1 and 3.4), and near fixation, the drive is itself resistant to invasion (SI Sections 3.2 and 3.5). Furthermore, fully-resistant populations are also susceptible (SI Sections 3.3 and 3.6), implying that the drive wins in any resident population. If, alternatively, the drive is costly and resistance is less costly (Regime IV), both the gene drive and resistant alleles go extinct (Fig. 2c and 3d). More precisely, wild-type populations are immune to invasion (SI Sections 3.1 and 3.4), while drive populations are susceptible to invasion by the resistant allele (SI Sections 3.2 and 3.5), and resistant populations are susceptible to invasion by the wild-type allele (SI Sections 3.3 and 3.6).

The other two regimes, II and III, yield counterintuitive and previously unreported behavior. Of particular interest is Regime II, wherein the drive is costly but resistance is costlier.

Here we observe what we term threshold-dependent drive fixation (Fig. 2c and Fig. 3b). If the drive is introduced at a sufficiently high frequency in a wild-type population, it goes to fixation, otherwise the population returns to its initial wild-type state. Mathematically, this is due to bistability: wild-type populations are immune to invasion (SI Sections 3.1 and 3.4), but so are populations with a fixed drive allele (SI Sections 3.2 and 3.5). The boundary between these two behaviors then manifests itself as a threshold (which we refer to as the 'invasion threshold') (Fig. 2c). On the other hand, if the drive is fairly neutral with resistance even more-so (Regime III), then we observe coexistence of all three alleles (Fig. 2c and Fig. 3c). This behavior can again be explained by the stability of the various fixed points—each allele, at fixation, is susceptible to invasion by at least one of the other alleles (SI Sections 3.1-3.6). Regardless of initial conditions, the system spirals into an interior fixed point (given in SI Section 5) which appears to be stable.

Next we consider how these dynamics vary within the regimes themselves. Toward this aim, we have taken the two most useful regimes—I and II—and studied their most salient features: the speed of drive spread (Fig. 4a) and the invasion threshold (IT) (Fig. 4b). To quantify the former, we calculate the time before the drive allele reaches a frequency of 90%, which we denote t_{90}. Intuitively, this decreases as the drive becomes more neutral and as resistance becomes more costly (Fig. 4a), while increasing the conversion probability P increases the size of the regime over which fixation occurs (Fig. 2b) and speeds up drive fixation for set costs (Fig. 4a). The invasion threshold in Regime II is less intuitive: the resistance cost affects whether the threshold behavior occurs at all but does not appreciably affect the value of the threshold (Fig. 4b), while the threshold does increase with the drive cost, from nearly IT=0 at the lower boundary (c=P/(1+P)) to IT=1 as the drive approaches lethality (c=1). Again, the conversion probability P simply determines the size of the regime over which threshold behavior occurs.

Our results suggest that gene drive resistance—not considered in any depth previously—must be thoroughly understood before the technology reaches real-world application. Most important is the possibility of 'cost-free resistance'. If an organism evolves resistance through a mechanism which bears no cost, for example a synonymous mutation in the Cas9 protospacer sequence, a fourth allele will emerge which is constrained to the horizontal (s=0) axis in Figure 2a, and this allele will always out-compete the gene drive at equilibrium. Indeed, this effect—drive fixation followed by extinction—has been observed in taxonomic and phylogenetic analyses of natural homing endonuclease genes[26,27]. To address this problem, drive resistance could likely be delayed, although not entirely precluded, by the use of an RNA-guided gene drive system employing multiple guide RNAs which all target a particular locus, as suggested by Esvelt et al[2]. If cutting were induced by two or more guides simultaneously, then repair by NHEJ would result in a loss of the intervening sequence and disrupt target gene function. This strategy, while intuitively appealing, should be validated by further theoretical study.

In contrast to the canonical goal of gene drives—to spread as effectively as possible—there are also applications for which containment to a local population is required. For example, the mosquito *Culex quinquefasciatus* is invasive to Hawaii and, as the principal vector for avian malaria, has been implicated in the extinction of a variety of endemic avian species[28]. Thus it might be a desirable goal to locally eradicate or otherwise modify Hawaiian *C. quinquefasciatus* without affecting its native populations elsewhere. Toward this aim, a gene drive system could be engineered to exist in our Regime II (Fig. 2 and Fig. 3b) and would naturally constitute a threshold drive: assuming that the flux of mosquitos from Hawaii to other populations is sufficiently low, any escaped drive allele would go extinct upon arrival. Previously considered methods for constructing such drives—based on engineered underdominance or toxin-antidote

systems—require high introduction frequencies to spread in the intended population and ignore the problem of drive resistance[11,12]; thus we believe our method to be a significant advance toward the engineering of threshold-based gene drives.

Methods

Evolutionary dynamics model

Throughout this work we study a genetics-based evolutionary dynamics model; to avoid making any explicit allele frequency assumptions, we first consider the evolution of six types of diploid individuals, x_{AA}, x_{DD}, x_{RR}, x_{AD}, x_{RD}, and x_{RA}, where A, D, and R correspond to the wild-type, gene drive, and resistant alleles as described above. We enforce a density constraint such that, at any given time, the total number of individuals sums to one. In this way, we track the frequencies of the various individuals rather than their total abundances.

In the Supplementary Information (Section 1) we derive a continuous-time model for the evolutionary dynamics of this population assuming (1) an infinitely large population, (2) random mating, (3) standard segregation of allele pairs at meiosis, unless an individual is AD, in which case gametes receive a D allele with probability ½(1+P) or an R allele with probability ½(1-P), and (4) selection dynamics as described in Fig. 1d. This continuous-time model makes no explicit assumptions regarding allele frequencies, but our simulations show that it is equivalent to a simpler model (derived from the individual-based model) where we instead track the allele frequencies with explicit Hardy-Weinberg frequency assumptions; this suggests that the assumptions are valid, and thus we consider the allele-based model throughout the results presented in the main text, reducing the dimensionality of the system from five (six types of individuals with the density constraint) to two (three alleles with a density constraint).

In this simpler model, we consider the frequencies of the A, D, and R alleles, denoted p, q, and r respectively. In continuous time, these follow

$$\frac{dp}{dt} = \varphi[p^2 + pr - \varphi p]$$
$$\frac{dq}{dt} = \varphi[(1-c)(1+P)pq + (1-c)q^2 + (1-c)rq - \varphi q]$$
$$\frac{dr}{dt} = \varphi[(1-c)(1-P)pq + (1-s)r^2 + (1-c)rq + rp - \varphi r],$$

where φ is chosen to enforce our density constraint p+q+r=1.

Invasion and stability of fixed points

To the system of differential equations above, we make the substitution p=1-q-r. Then the (autonomous) system above is described by

$$\begin{cases} \frac{dq}{dt} = f_q(q,r) \\ \frac{dr}{dt} = f_r(q,r). \end{cases}$$

We Taylor expand to linearize the system near a given fixed point (q^*,r^*) and consider the Jacobian, given by

$$J_{(q^*,r^*)} = \begin{pmatrix} \left.\frac{\partial f_q}{\partial q}\right|_{(q^*,r^*)} & \left.\frac{\partial f_q}{\partial r}\right|_{(q^*,r^*)} \\ \left.\frac{\partial f_r}{\partial q}\right|_{(q^*,r^*)} & \left.\frac{\partial f_r}{\partial r}\right|_{(q^*,r^*)} \end{pmatrix}.$$

To determine the conditions for which allele invasion occurs in various resident populations, we then perform linear stability analysis of fixed points via consideration of the eigenvalues of the Jacobian. In particular, we consider the fixed points corresponding to wild-type fixation (0,0),

drive fixation (1,0), and resistant allele fixation (0,1). When an eigenvalue is zero and linear stability analysis is inconclusive, we also perform perturbation analysis to determine the invasion conditions (see Supplementary Information).

Parameter values for main text figures

Fig. 2a: an intermediate conversion probability was chosen, P=0.5. Fig. 2c: the conversion probability P was as in panel a, P=0.50. Cost parameters were chosen to most clearly illustrate the behaviors in the four regimes. Regime I: c=0.20, s=0.55, Regime II: c=0.40, s=0.55, Regime III: c=0.15, s=0.09, Regime IV: c=0.40, s=0.09. Fig. 3: here all parameters are as in Fig. 2c, with initial drive frequencies q_0 as follows. Regime I: q_0=0.01, Regime II: q_0=0.20 and q_0=0.40, Regime III: q_0=0.01, Regime IV: q_0=0.40. In each case, we set the initial wild-type allele frequency to one minus the initial drive frequency with no resistant allele. Fig. 4, Top: all parameters were chosen identically to the corresponding panels (Regime I and Regime II) in Fig. 3. Middle: P=0.25, Bottom: P=0.90. Throughout panel a, we use q_0=0.01. In Fig. 4b, we determined the invasion threshold for each (c,s) pair using a binary search-type numerical algorithm which identifies the threshold down to a resolution of r (r=0.01). More precisely, we initialize variables L=0 and U=1 and run a simulation with an initial drive frequency mid-way between U and L, q_0=(U-L)/2 (with the initial wild-type frequency being 1-q_0). If after T=200 the drive frequency is higher than its initial value, we consider q_0 to be above the threshold and set U=(U-L)/2. Otherwise we consider q_0 to be below the threshold and set L=(U-L)/2. The algorithm then continues recursively until $|L-U|<r$, at which point we make the approximation that the threshold occurs at q_0=(U-L)/2.

1. Burt, A. Site-specific selfish genes as tools for the control and genetic engineering of natural populations. *Proc. Biol. Sci.* **270,** 921–928 (2003).

2. Esvelt, K. M., Smidler, a. L., Catteruccia, F. & Church, G. M. Concerning RNA-guided gene drives for the alteration of wild populations. *Elife* **3,** e03401 (2014).

3. Mali, P., Esvelt, K. M. & Church, G. M. Cas9 as a versatile tool for engineering biology. *Nat. Methods* **10,** 957–63 (2013).

4. Gantz, V. M. & Bier, E. The mutagenic chain reaction: A method for converting heterozygous to homozygous mutations. *Science (80-.).* (2015). doi:10.1126/science.aaa5945

5. DiCarlo, J. E., Chavez, A., Dietz, S. L., Esvelt, K. M. & Church, G. M. *RNA-guided gene drives can efficiently bias inheritance in wild yeast. bioRxiv* (Cold Spring Harbor Labs Journals, 2015). doi:10.1101/013896

6. Windbichler, N. *et al.* A synthetic homing endonuclease-based gene drive system in the human malaria mosquito. *Nature* **473,** 212–215 (2011).

7. Windbichler, N. *et al.* Homing endonuclease mediated gene targeting in Anopheles gambiae cells and embryos. *Nucleic Acids Res.* **35,** 5922–33 (2007).

8. Gurwitz, D. Gene drives raise dual-use concerns. *Science (80-.).* **345,** 1010 (2014).

9. Oye, K. A. *et al.* Regulating gene drives. *Science (80-.).* **345,** 626–8 (2014).

10. Akbari, B. O. S. *et al.* Safeguarding gene drive experiments in the laboratory. *Science (80-.).* science.aac7932– (2015). doi:10.1126/science.aac7932

11. Akbari, O. S. *et al.* A synthetic gene drive system for local, reversible modification and suppression of insect populations. *Curr. Biol.* **23,** 671–7 (2013).

12. Marshall, J. M. & Hay, B. a. Confinement of gene drive systems to local populations: A comparative analysis. *J. Theor. Biol.* **294,** 153–171 (2012).

13. Sinkins, S. P. & Gould, F. Gene drive systems for insect disease vectors. *Nat. Rev. Genet.* **7,** 427–435 (2006).

14. Charlesworth, B. & Langley, C. H. The population genetics of Drosophila transposable elements. *Annu. Rev. Genet.* **23,** 251–287 (1989).

15. Chen, C.-H. *et al.* A Synthetic Maternal-Effect Selfish Genetic Element Drives Population Replacement in Drosophila. *Science (80-.).* **316,** 597–600 (2007).

16. Lyttle, T. W. Segregation distorters. *Annu. Rev. Genet.* **25,** 511–557 (1991).

17. Mali, P. *et al.* RNA-guided human genome engineering via Cas9. *Science* **339,** 823–6 (2013).

18. Simoni, A. *et al.* Development of synthetic selfish elements based on modular nucleases in Drosophila melanogaster. *Nucleic Acids Res.* **42,** 7461–72 (2014).

19. Deredec, A., Burt, A. & Godfray, H. C. J. The population genetics of using homing endonuclease genes in vector and pest management. *Genetics* **179,** 2013–2026 (2008).

20. Deredec, A., Godfray, H. C. J. & Burt, A. Requirements for effective malaria control with homing endonuclease genes. *Proc. Natl. Acad. Sci. U. S. A.* **108,** E874–80 (2011).

21. Khanna, K. K. & Jackson, S. P. DNA double-strand breaks: signaling, repair and the cancer connection. *Nat. Genet.* **27,** 247–254 (2001).

22. Vilenchik, M. M. & Knudson, A. G. Endogenous DNA double-strand breaks: production, fidelity of repair, and induction of cancer. *Proc. Natl. Acad. Sci. U. S. A.* **100,** 12871–12876 (2003).

23. Mao, Z., Bozzella, M., Seluanov, A. & Gorbunova, V. Comparison of nonhomologous end joining and homologous recombination in human cells. *DNA Repair (Amst).* **7,** 1765–71 (2008).

24. DiCarlo, J. E. *et al.* Genome engineering in Saccharomyces cerevisiae using CRISPR-Cas systems. *Nucleic Acids Res.* **41,** 4336–43 (2013).

25. Griffiths, A. J. F. *An Introduction to Genetic Analysis*. (W. H. Freeman, 2005). at <[redacted]>

26. Burt, A. & Koufopanou, V. Homing endonuclease genes: the rise and fall and rise again of a selfish element. *Curr. Opin. Genet. Dev.* **14,** 609–15 (2004).

27. Goddard, M. R. & Burt, A. Recurrent invasion and extinction of a selfish gene. *Proc. Natl. Acad. Sci.* **96,** 13880–13885 (1999).

28. Iii, C. V. R., Riper, S. G. Van, Goff, M. L. & Laird, M. The Epizootiology and Ecological Significance of Malaria in Hawaiian Land Birds. *Ecol. Monogr.* **56,** 327–344 (1986).

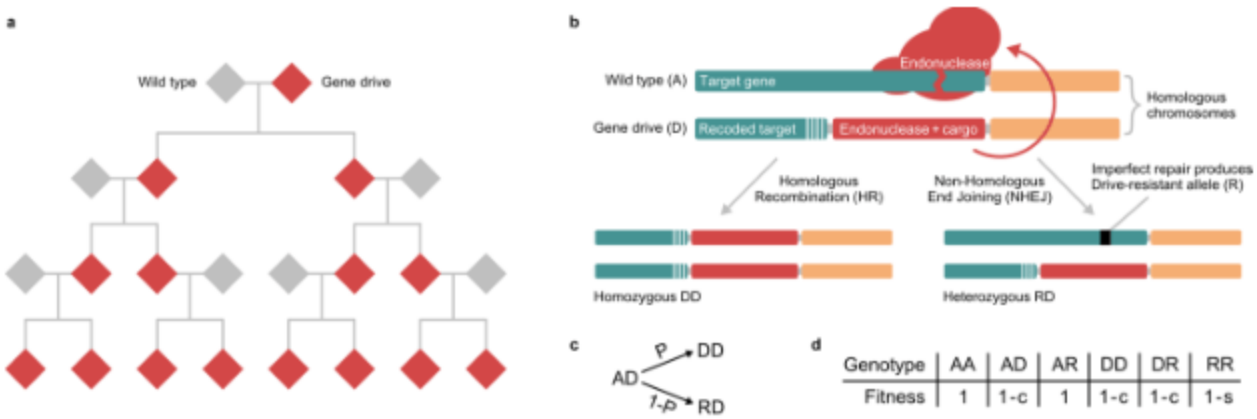

Figure 1 | Endonuclease gene drives undergo biased inheritance in wild populations. a, Matings between wild type (AA) and gene drive (DD) individuals yield homozygous DD offspring, allowing for rapid spread of the gene drive allele. **b**, This is accomplished by conversion of heterozygous AD cells to homozygous DD cells in the early embryo or late germline. The gene drive carries an endonuclease (red) which cuts the wild type allele at its own position on a homologous chromosome (blue). Homologous recombination (HR) then uses the drive chromosome as a template to repair the break, inserting a new drive construct at the break site. Alternatively, repair by non-homologous end joining (NHEJ) produces a small insertion/deletion mutation, protecting the site from future recognition by the endonuclease. **c**, Our model abstracts this process using a parameter P which is roughly the probability of repair by HR. **d**, We assume that the gene drive has a dominant fitness cost c, while resistant alleles have a recessive fitness cost s.

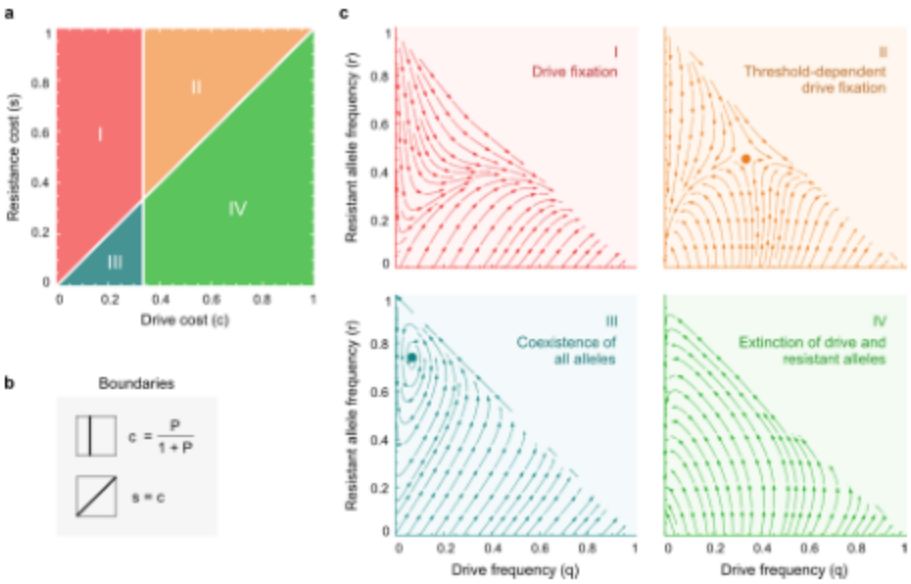

Figure 2 | The relative fitness costs of the gene drive (c) and the resistant allele (s) determine four distinct long-term behaviors. a, Phase diagram depicting the regimes in which each of the four behaviors occur. **b**, The phase boundaries in **a**. The vertical boundary is determined by the probability of successful repair by HR, while the diagonal boundary divides the space based on which fitness cost is greater. **c**, Representative phase portraits for each regime.

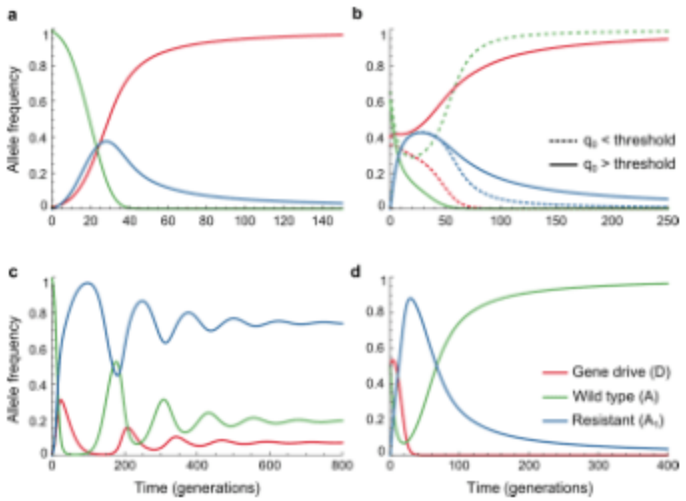

277

278 **Figure 3 | The four regimes in Fig. 2 produce diverse dynamic behaviors.** Example simulations depicting allele
279 frequencies of the gene drive (red), wild-type (green), and resistant alleles (blue) for each of the regimes in Fig. 2. **a**
280 through **d** demonstrate Regimes I through IV, respectively. In **b**, two simulations are depicted: one with an initial
281 gene drive frequency below the invasion threshold (dashed lines) and one above (solid lines).

282

283

284

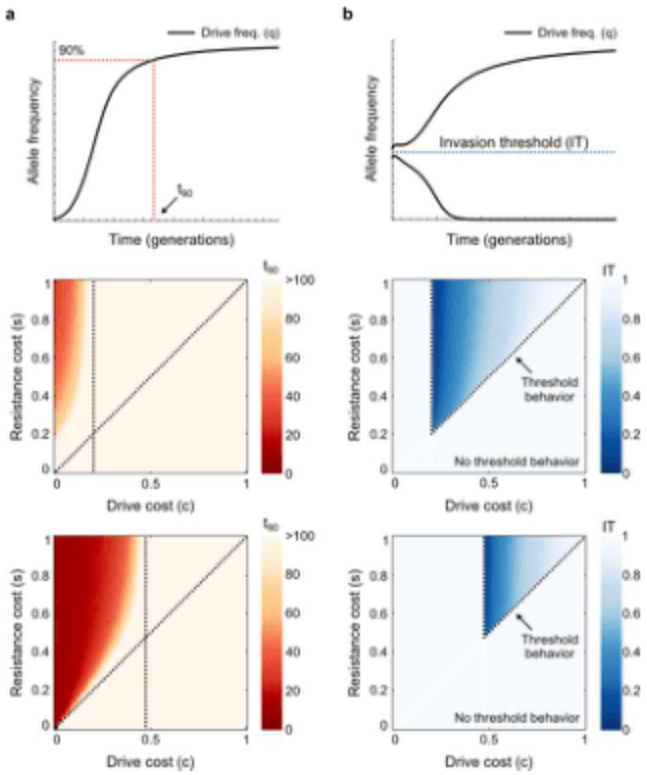

Figure 4 | The speed of gene drive spread and the invasion threshold are both tunable based on the fitness costs of the gene drive (c) and the resistant allele (s). a, The time (in generations) before a gene drive reaches a frequency of 90%, denoted t_{90} (illustrated at top, red). Pictured below are heat maps of t_{90} as a function of the drive cost and resistance cost for organisms having low (middle, P = 0.25) or high HR rates (bottom, P = 0.90). **b**, The invasion threshold, denoted IT, for drives in Regime II (illustrated at top, blue). Below are heat maps for organisms with low (middle, P = 0.25) or high HR rates (bottom, P = 0.90). Dashed black lines represent the regime boundaries in Fig. 2b.